Stability analysis of relativistic magnetized astrophysical jets

HELLENIC REPUBLIC
National and Kapodistrian University of Athens

Charalampos Sinnis, Nektarios Vlahakis

Section of Astrophysics, Astronomy & Mechanics
Department of Physics, National and Kapodistrian University of Athens
chsinnis@phys.uoa.gr, vlahakis@phys.uoa.gr

Abstract

Astrophysical jets are observed as stable structures, extending in lengths several times their radii. The role of various instabilities and how they affect the observed jet properties has not been fully understood. Using the ideal relativistic MHD equations to describe jet dynamics we aim to study the stability properties through linear analysis. Our jets' physical quantities are defined by the acceleration and collimation processes near the central object that generates the outflow. So, the distribution of each quantity carries the signature of the processes taking place at the early stages of jet propagation. In order to find the growth rates for the instabilities we solve numerically the perturbed system. We find connections between growth rates and various characteristic parameters such as magnetization, as well as the underlying dominating physical mechanism that trigger the instabilities, whether it is a matter- or magnetic field-dominated process.

1. Theoretical framework

- Two main categories of instabilities:
  Kelvin–Helmholtz type $\rightarrow$ shear velocity profile or fluids in contact with different velocities(e.g. some solutions in [2]).
  Current–driven $\rightarrow$ helical magnetic field (e.g. in [1])
  Stability properties of outflows through a linear stability analysis.
- Jet dynamics described by ideal relativistic magnetohydrodynamics (RMHD).
- Jets have to be in force equilibrium along the radial direction, i.e., the radial component of the momentum equation must be satisfied:

$$\gamma\rho_0\left(\mathbf{v}\cdot\nabla\right)\left(\xi\gamma\mathbf{v}\right) = -\nabla P + \frac{J^0\mathbf{E}+\mathbf{J}\times\mathbf{B}}{c} \tag{1}$$

  where, γ is the Lorentz factor, $\mathbf{v}$ the bulk flow velocity, ρ_0 is the proper density and $\xi = 1 + \frac{\Gamma}{\Gamma-1}\frac{P}{\rho_0 c^2}$ is the specific enthalpy. Also, P is the thermal pressure, $J^0/c,\ \mathbf{J}$ are the electric charge and current densities, and finally $\mathbf{E}\ ,\mathbf{B}$ the electric and the magnetic fields.
- Jets are in equilibrium with their environment, which is assumed to be a stationary unmagnetized medium.
- Small perturbations are of the form:
  $\delta Q = Q_1(\varpi)exp\left[i\left(m\phi + kz - \omega t\right)\right]$, with $|Q_1| \ll |Q_0|$.
- $\omega = \Re\omega + i\Im\omega \in \mathbb{C}$. This leads to a time–dependent amplitude for the perturbations. Whenever $\Im\omega > 0$ we have an unstable mode with growth timescale $\frac{1}{\Im\omega}$.
- The final linearized set of equations is a 2x2 first order complex differential equation system.
- Our main goal is to find the dispersion relation of the system, $\omega = \omega(k)$.

2. Jet models

Model is cylindrical, steady–state and axisymmetric, so the unperturbed physical quantities depend only on the cylindrical radius ϖ. The special point of this study is that the physical quantities' functional dependence on the radius is shaped by the acceleration and collimation processes near the central object that creates the outflow [3, 4].
As for the physical quantities we assume a slowly cold rotating jet, i.e. $\xi = 1 \Rightarrow P = 0$. Hence, the total pressure (Π) is related only to the magnetic fields through the relation $\Pi = \frac{B^2-E^2}{2} \equiv \frac{F}{2}$.
The functional behavior of the physical quantities is summarised below:

$$\gamma = \begin{cases}\gamma_a, & \varpi \ll \varpi_j \\ \gamma_b, & \varpi \simeq \varpi_j\end{cases} \qquad \upsilon_\phi \ll \upsilon_z$$

$$B_z \propto \begin{cases} b_1, & \varpi \ll \varpi_j \\ 1/\varpi, & \varpi \simeq \varpi_j\end{cases} \qquad B_\phi \propto \begin{cases}\varpi, & \varpi \ll \varpi_j \\ 1/\varpi, & \varpi \simeq \varpi_j\end{cases}$$

where $\gamma_a > \gamma_b,\ b_1$ are constants. The methodology we used demands that the configurations obey Ferraro's law and the radial component of (1) below:

$$\chi = \upsilon_\phi - \frac{\upsilon_z B_\phi}{B_z} \tag{2}$$

$$\frac{B_\phi^2 - E^2}{\varpi} - \rho\frac{\gamma^2\upsilon_\phi^2}{\varpi} + \frac{d\Pi}{d\varpi} = 0 \tag{3}$$

where $\chi = \frac{\varpi\Omega}{c}$. For this specific modelling of the jet we define the physical quantities' profiles to be:

$$\upsilon_\phi = \frac{\lambda\chi}{1+\lambda\chi^2} \qquad F = \frac{B_0^2}{1+Ky^2}$$

$$\gamma = \gamma_b + \frac{\gamma_a - \gamma_b}{1+Qy^2} \quad B_z = \frac{B_0}{1+y^2}$$

where $y = \frac{\varpi}{\varpi_0}$ and B_ϕ is given by:

$$B_\phi = -\sqrt{F + (\chi^2-1)B_z^2}$$

Finally, solving (3) for ρ completes the algorithm and we have the profiles of every physical quantity needed, in order to define the unperturbed state of the jet.
The parameter space is given by:

γ_a = 10 $\quad\gamma_b$ = 2,5,8 $\quad\lambda$ = 0.0004
Q = 10 K = 0.99, 0.9

So, $\gamma_a,\ \gamma_b$ are the Lorentz factor values on the axis and the boundary of the jet respectively. Parameter λ controls the maximum value for υ_ϕ. K controls the maximum magnetization for the jet, the lower the value for K gets, the lower the maximum magnetization becomes. Q affects the radius where the profile of the Lorentz factor begins it's decrease and finally $\varpi_0 = \frac{\gamma c}{\Omega}|_{axis}$.
In Fig. 1 we see an overview for the unperturbed state of the jet. Apart from the quantities that we defined, it is helpful to focus on the density and magnetization profile respectively. For the first one we can see that in the area surrounding the axis the profile is almost constant, then it proceeds to increase up to a specific value and finally it decreases many orders of magnitude compared to the value on the axis. In contrast, the magnetization near the axis of the jet has $\sigma < 1$ meaning that the magnetization of the jet is rather weak. Then towards the boundary of the jet the magnetization increases rapidly acquiring it's maximum on the boundary of the outflow. Just to note that the density of the external medium is 100 times the density of the jet measured on axis.

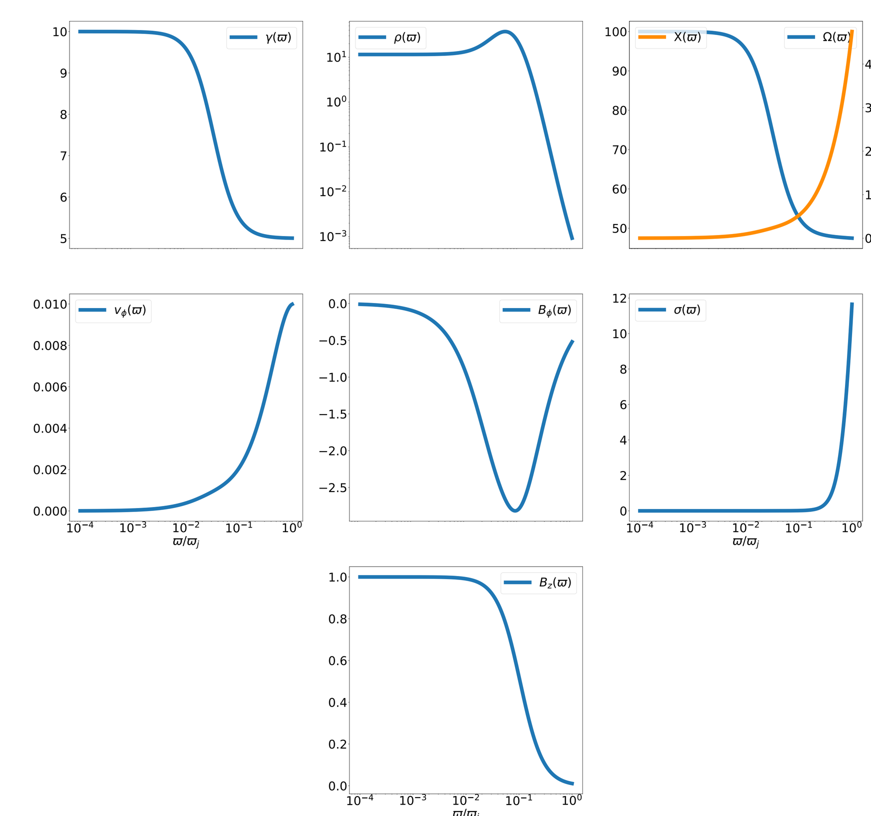

Figure 1: *Jet configuration overview for $\gamma_b = 5,\ K = 0.99$.*

3. Methodology

We solve numerically the linearized differential equations using a shooting method algorithm. We provide the algorithm with:
- differential equations
- boundary conditions defined on the axis, at the jet–environment interface and at great distances $(r \rightarrow \infty)$
- The solutions in the environment are Bessel functions.

The last piece of information is an initial "guess" for $\Re(\omega)$, and $\Im(\omega)$ at a given k in order to begin the shooting method.

4. Results

Our results will focus on the behavior of the $\Im\omega$ versus the parameters of importance. The first parameters are γ_b and σ_{max} which is the maximum magnetization of each configuration. $\Im\omega$ has units of c/ϖ_j which is the inverse of the light crossing time of jet's radius.

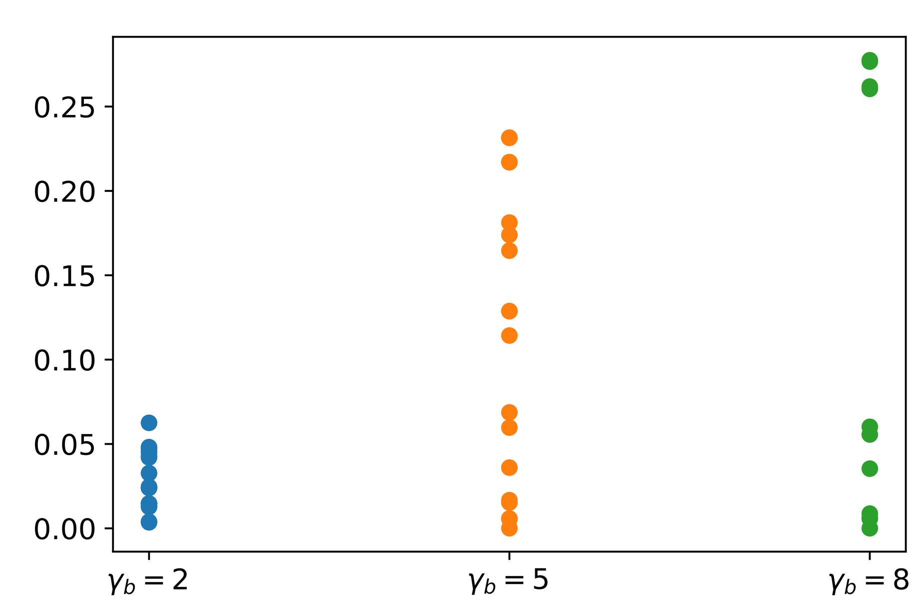

Figure 2: *Plot for the maximum $\Im\omega$ versus γ_b for every solution. There is correlation between the value of γ_b and the values of $\Im\omega$.*

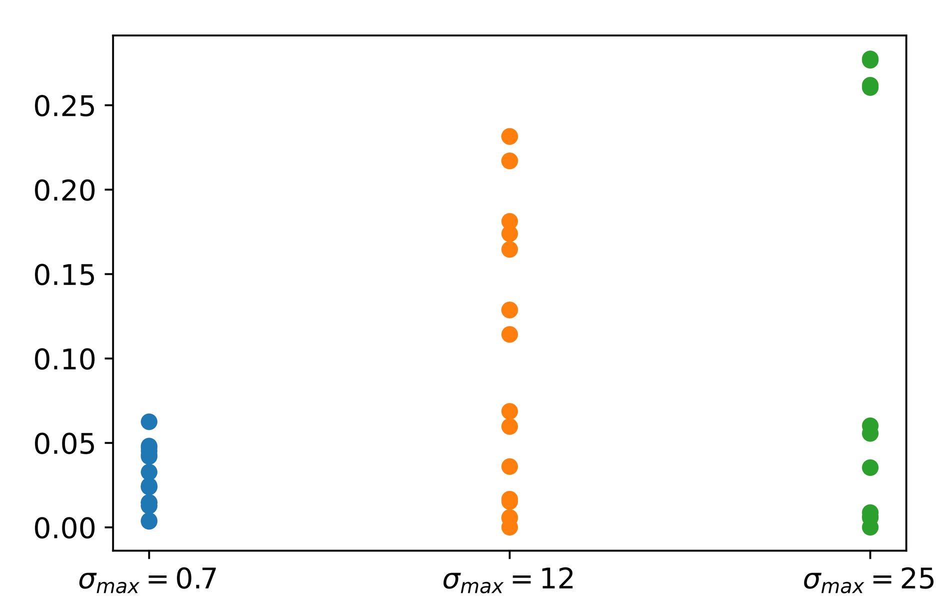

Figure 3: *Plot for the maximum $\Im\omega$ versus σ_{max} for every solution. As magnetization increases the jet becomes more unstable.*

In Fig. 2, 3 we depict the distribution of $\Im\omega$ versus γ_b and σ_{max} respectively. We observe that for both plots, when the respective parameter increases, also the $\Im\omega$ increases. This fact could imply both Kelvin–Helmholtz and current-driven mechanisms affecting the outcome. For the first mechanism the increasing velocity difference at the boundary of the jet enhances Kelvin–Helmholtz instability, while for the latter counterpart the increasing magnetization strengthens the current-driven mechanism.
In order to understand better the configuration's main mechanism we study the fiducial case, setting different value for K. The new value was set to $K = 0.9$ leading to a different maximum magnetization $\sigma_{max} \approx 1$. The corresponding values of $\Im\omega$ decreased at approximately $0.01\varpi_j/c$. This result demystifies the situation, setting the current-driven scenario as the most probable. This is based on the fact that the timescales became larger than the ones found for the same case with $K = 0.99$, meaning that the change in the magnetization is the reason for the change in $\Im\omega$. For both K cases the velocity profile does not change.
In order to further investigate the physical mechanism we plot in Fig. 4 and in Fig. 5 the real part of the radially-dependent part of the perturbations of the physical quantities and also the real part of the distribution of radial components of perturbed forces acting on the jet respectively. Both plots include the real parts of the quantities. The perturbed quantities, apart from $\upsilon_{1\varpi}$, become maximum near the axis of the outflow. As radius increases the distributions become negligible. This indicates that the most active region of the jet, in terms of instabilities' development, are the regions for $\varpi \ll \varpi_j$. Also, the dominant component for the magnetic field is the toroidal. Hence, the perturbation of the magnetization and the poloidal current are going to be important, relating the instability to the current-driven mechanism once more.
In Fig. 5 clearly the electromagnetic force is dominant over the inertial related counterpart. The Lorentz force is given by $(\boldsymbol{J} \times \boldsymbol{B})_1$ and the inertial by $[\gamma\rho(\boldsymbol{\upsilon}\cdot\nabla)(\gamma\boldsymbol{\upsilon})]_1$, excluding the centrifugal force, which are negligible either way, due to small values for υ_ϕ. So, the current-driven scenario mechanism is favoured, also, from this result.

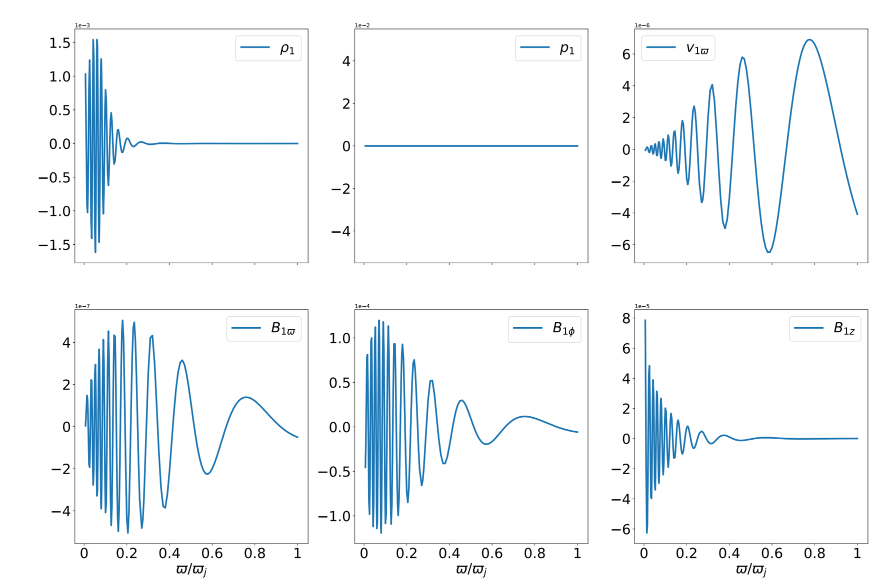

Figure 4: *Real part of the perturbed physical forces versus radius. From left to right in top row are the density, thermal pressure and radial component of velocity. Bottom row are the poloidal, toroidal and radial component of magnetic field.*

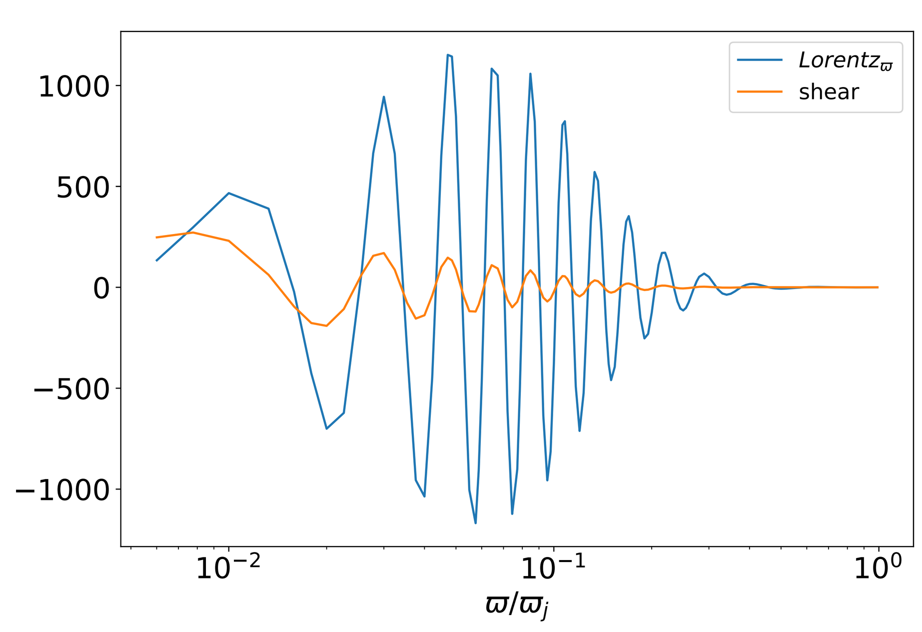

Figure 5: *Real part of the radial distribution of perturbed forces acting on the jet. Blue and orange lines are the radial components of Lorentz force and inertial forces respectively.*

References

[1] G. Bodo, G. Mamatsashvili, P. Rossi, and A. Mignone. Linear stability analysis of magnetized relativistic jets: the non-rotating case. *MNRAS*, 434(4):3030–3046, 2013.
[2] J. Kim, D. S. Balsara, M. Lyutikov, and S. S. Komissarov. On the linear stability of sheared and magnetized jets without current sheets - relativistic case. *MNRAS*, 474(3):3954–3966, 2018.
[3] S. S. Komissarov, N. Vlahakis, A. Königl, and M. V. Barkov. Magnetic acceleration of ultrarelativistic jets in gamma-ray burst sources. *MNRAS*, 394(3):1182–1212, 2009.
[4] N. Vlahakis. Ideal Magnetohydrodynamic Solution to the σ Problem in Crab-like Pulsar Winds and General Asymptotic Analysis of Magnetized Outflows. *APJ*, 600(1):324–337, 2004.

Acknowledgements

Ευρωπαϊκή Ένωση European Social Fund
Operational Programme Human Resources Development, Education and Lifelong Learning
Co-financed by Greece and the European Union
ΕΣΠΑ 2014-2020

This research is co-financed by Greece and the European Union (European Social Fund-ESF) through the Operational Programme «Human Resources Development, Education and Lifelong Learning» in the context of the project "Strengthening Human Resources Research Potential via Doctorate Research" (MIS-5000432), implemented by the State Scholarships Foundation (IKY)